Chapter 9
Current Arraying Capabilities

Arraying has been utilized in the DSN a number of times over the past several years. The Voyager Mission relied on arraying to increase its data return during Uranus encounter in 1986 and Neptune encounter in 1989 [1,2]. More recently, the Galileo Mission also benefited from arraying to significantly increase the science data return in the face of the failure of the spacecraft's main communications antenna. Galileo arraying employed up to five antennas, located at three different tracking facilities and spread over the two continents of North America and Australia. Arraying alone resulted in a factor of 3 improvement in data return. [3– 5]

While baseband arraying was used in the earlier missions, full-spectrum arraying was employed for the first time in the DSN during the Galileo Mission. The Galileo arraying equipment, however, was tailored to low data rates (below 1 ksym/s). More recently, a new capability has been implemented that extends the supported data rate for full-spectrum arraying to 6 Msym/s. Unfortunately, because of the high transmission bandwidth between the antennas required to sustain these high data rates, the array is limited to those antennas within a tracking complex, i.e., no intercomplex arraying across two continents is supported. It is this implementation of arraying in the DSN, referred to as the array portion of the Full Spectrum Processing Subsystem (FSPS)—or the Full Spectrum Processing Array (FSPA)—that is described below. This subsystem is expected to provide arraying capability for the DSN in the future. While the FSPA is nominally intended for 34-m antennas, it is capable of arraying any size of antenna, including combinations of 70-m and 34-m antennas, up to 6 antennas (expandable up to a maximum of 8 antennas). The original subsystem was implemented only at the Goldstone Complex. It will be available for arraying up to 4 antennas (again, expandable up to

8 antennas) at the end of 2003 at the overseas complexes (Madrid, Spain, and Canberra, Australia).

9.1 Equipment Description

Signal processing for full-spectrum arraying is accomplished in two main assemblies—the Full Spectrum Receiver (FSR) and the Full Spectrum Combiner (FSC; this acronym has previously been used to mean full-spectrum combining, but here is used to mean a particular piece of equipment, the Full Spectrum Combiner), pictured as two equipment racks in Fig. 9-1. The FSR inputs are individual 300-MHz intermediate frequency (IF) analog signals derived from the radio frequency (RF) signals that have been received by the antenna, amplified by low-noise front-end microwave equipment, and downconverted in frequency by an RF-to-IF downconverter. The FSR outputs are digitally sampled bands of 16-Msamples/s data. Once digitally combined by the FSC, the signal is converted back to analog form and upconverted to an intermediate frequency near to the original 300-MHz IF. Except for having an improved SNR, the signal is, in principle, identical to the signal that arrives at the particular array antenna designated as the reference. Downstream processing, such as demodulation, decoding, and range detection, then can be accomplished on this combined output to yield final science and engineering data products.

Fig. 9-1. FSPA signal processing equipment: the FSR on the left, and the FSC on the right.

Major components of the FSR are illustrated in Fig. 9-2. The analog-to-digital converter (A/D) and the digital downconverter capture a relevant portion of the 300-MHz IF analog signal in a 16-MHz band that is preserved as 8-bit sampled, in-phase (I) and quadrature-phase (Q) digital data streams. The delay line and phase rotator modules correct signal delay and phase using information from predicts together with feedback from the FSC-derived residuals. The signal monitor module samples the digital data streams and transforms them into measurements of carrier- and telemetry-signal SNRs. These values are transmitted to the operators for monitoring. They also are relayed to the FSC for proper setting of the combining coefficients. Measurement of the carrier-signal SNR is obtainable directly from the square of the standard Fourier transform of this signal. Measurement of the telemetry-signal SNR, however, requires some manipulation involving the correlation of the upper and lower harmonics of the telemetry subcarrier signals. The real-time and data processors handle high-level monitor and control in the FSR.

Figure 9-3 presents the major components of the FSC. The cross-correlation of upper and lower sideband signals of different antennas is used to derive differential phase and delay values for feedback to the FSRs. At the same time, the weight and sum module combines the weighted FSC input signals to produce optimal output. The digital-to-analog converter (D/A) and upconverter module performs the conversion of the digital baseband stream back to an analog 300-MHz IF. The signal monitor module as well as the real-time and data processors carry out functions similar to those in the FSR.

9.2 Signal Processing

This section will highlight some aspects of the signal processing used in the FSPA. The main focus is on correlation, delay compensation, and combining.

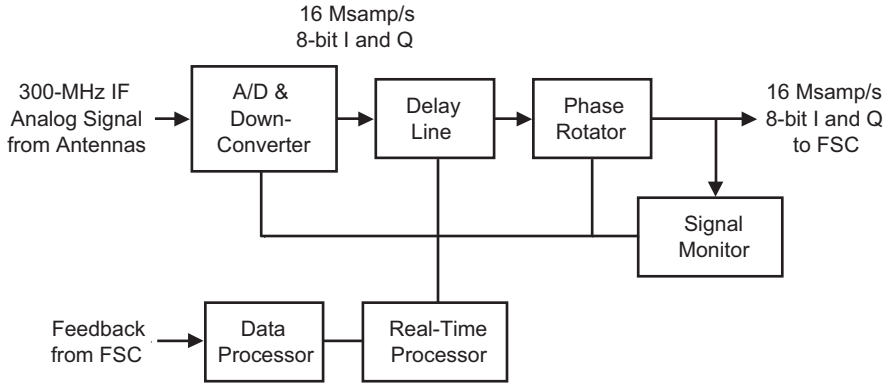

Fig. 9-2. Processing components in the FSR.

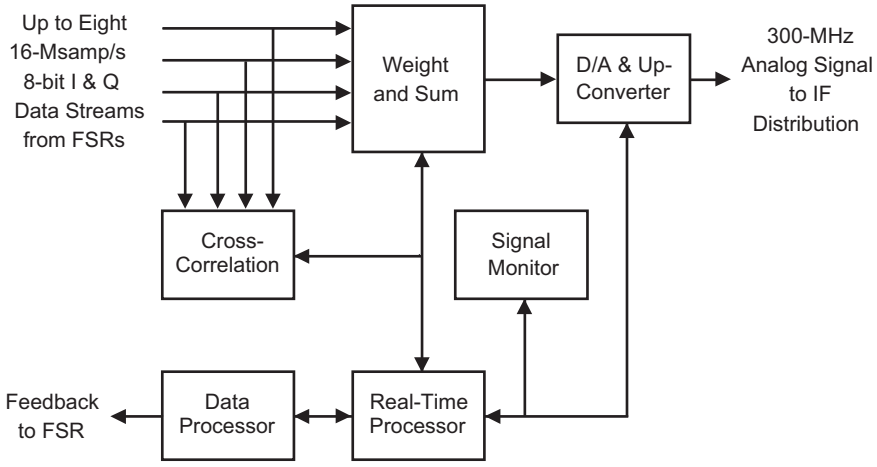

Fig. 9-3. Processing components in the FSC.

9.2.1 Correlation

The success of combining depends on good correlation results. Correlation is an essential process without which proper combining cannot be done. Figure 9-4 shows the accepted placement of filters relative to the type of signal received in order to extract the best phase and delay information. In the broadband case, it is possible to place the filters further apart if better delay precision is desired, provided that phase ambiguity is not a problem.

Figure 9-5 shows the details of the correlation processing [6]. With the aid of Doppler predicts, the upper and lower sidebands of the telemetry signal received at each antenna are captured in the FSR digital data streams. The upper sideband from one antenna then is correlated with the same component of the telemetry in the array reference antenna, from which the phase difference at the upper sideband is measured. The same process is performed simultaneously on the lower sideband signal component. As diagrammed in Fig. 9-6, an average of these two phase measurements then yields the phase offset, while the ratio of their difference to twice the sideband frequency provides the time delay.

As described in Chapter 8, there are different ways of implementing the correlation process. The FSPA equipment supports two approaches, both successfully tested. The simpler scheme (not surprisingly called Simple) involves choosing the antenna having the highest SNR as the reference, against which all other antenna signals are correlated. This scheme has been shown to work well when one element of the array has a significantly higher SNR than the others, as in the case of arraying the 70-m with one or more 34-m antennas.

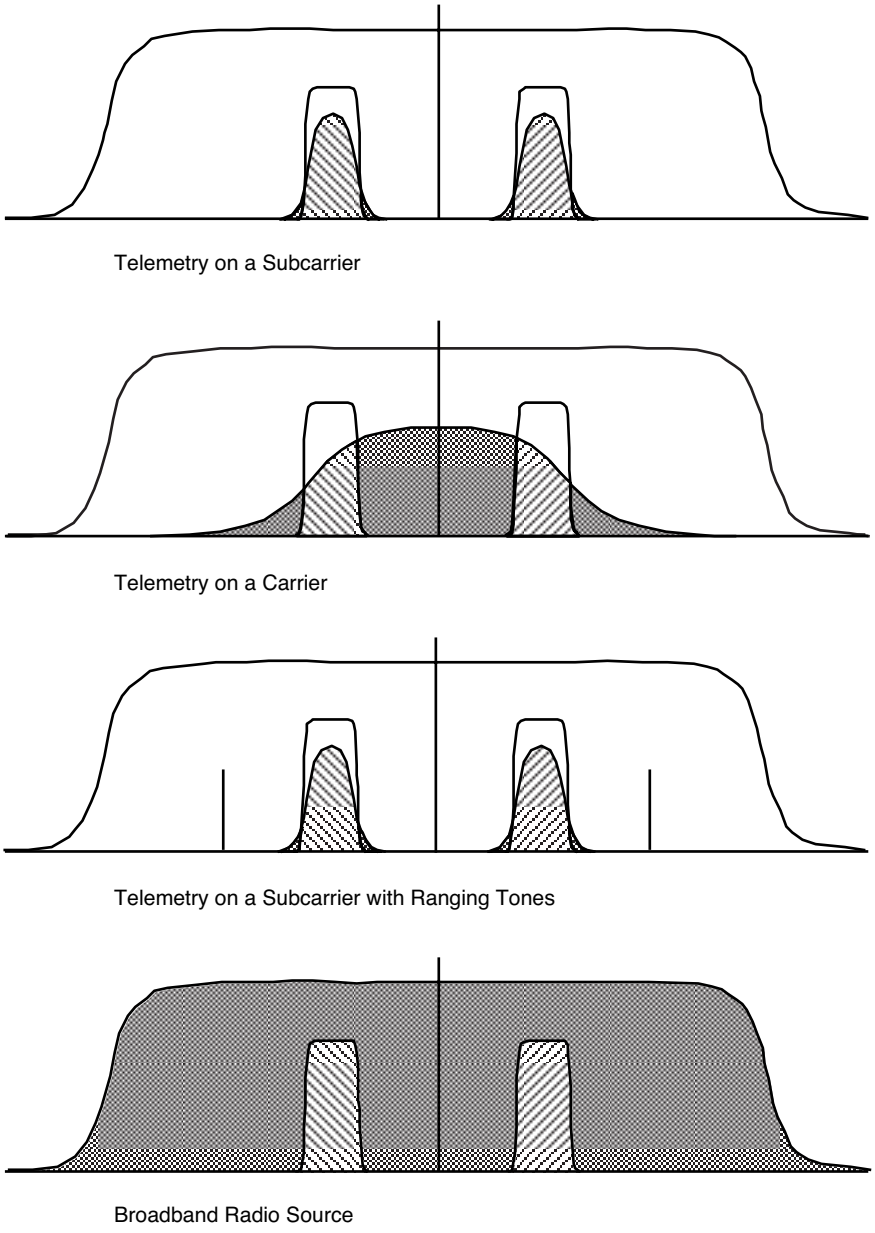

Fig. 9-4. Placement of filters for correlation of different signals.

The second method (called Sumple) treats as the reference a rotating sum of all antenna signals except the one under consideration. In other words, one antenna signal will be correlated against the sum of all the others. Simulation results presented in Chapter 8 indicate that the rotating sum method performs better

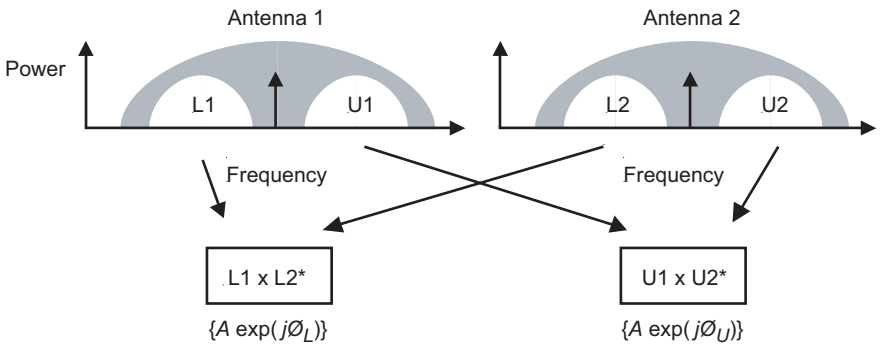

Fig. 9-5. Correlation processing.

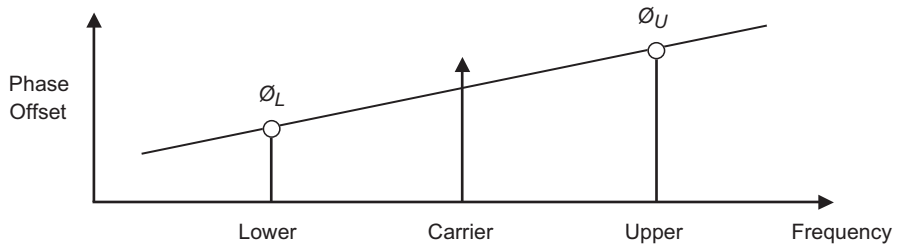

Phase Error = $(Ø_U + Ø_L) / 2$

Delay Error ~= $(Ø_U - Ø_L)$ / (2 x Sideband Frequency)

Fig. 9-6. Derivation of phase and delay errors.

than the fixed-reference method at a low SNR, and that the final solution emerges within a few iterations (see Fig. 8-3) [7]. The simulations also included a third approach using the Eigen value method [8] and a fourth approach, referred to as the Root-Mean-Square method. However, neither of these two algorithms was implemented in the FSC.

Consideration must be given to setting the optimum integration or averaging time in the correlation process. Based on thermal noise considerations, a long integration period is preferred since it would yield a phase estimate with small error. Obviously, the lower the signal level, the longer the integration time must be to achieve a given phase error. The problem, however, is that signals received at different antennas travel through different portions of the Earth's troposphere and, consequently, are subjected to varying delay. These tropospheric delays vary on a relatively short timescale, resulting in a deterioration of correlation for long integrations. An illustration is provided in Fig. 9-7 for a fixed combined symbol SNR at –5 dB/Hz, with equal aperture antennas separated by a baseline of 1 to 10 km [9,10]. At X-band, the

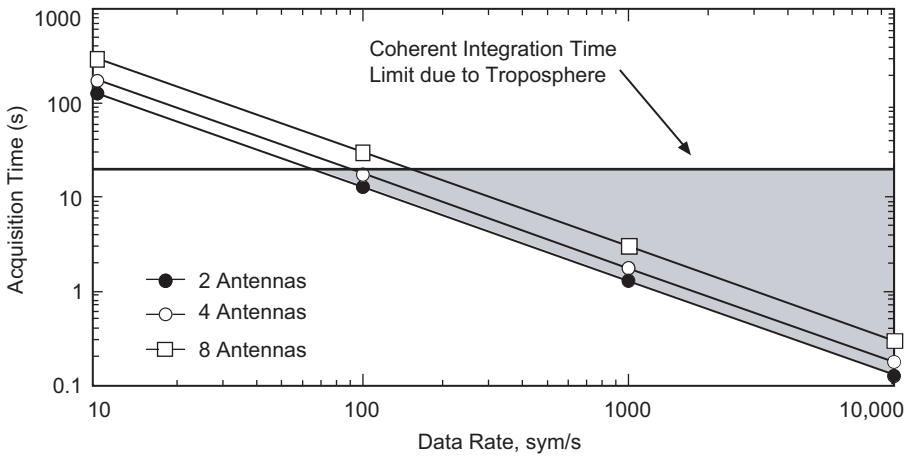

Fig. 9-7. Limits of correlation integration time.

tropospheric limit for a 20-deg phase-correlation error is about 20 seconds. The shaded triangular area is the operating region bounded by two constraints—thermal and tropospheric noise. Note also that the graph is expressed in terms of symbol rate, rather than in received SNR. Given a fixed symbol SNR, these two quantities are equivalent.

Care also must be taken in the use of correlation measurements to drive a feedback system. Invalid correlation results arise when one or both signals encounter problems. For example, one antenna could be mispointed or the spacecraft might go behind a planet. As in any control feedback system, it must deal with error signals that might drive the system away from a stable condition. Prevention of these types of problems can be achieved with appropriate filters on the FSC correlation estimates.

9.2.2 Delay Compensation

The delay compensation process is accomplished in two steps. In the first step, each FSR is provided with two sets of delay predicts—one for the various antennas being processed, the other for the reference antenna. These predicts have been computed (off-line, prior to the pass) from the spacecraft trajectory and the location of the tracking antennas. Using a model based on these predicts, the FSR removes a majority of the differential delay between any particular antenna and the reference antenna so that its signal can be aligned with the reference.

Over the course of an observing pass, the relative positions of different antennas in the array change with respect to the spacecraft. The delay of the non-reference signal varies relative to that of the reference. The relative delay is corrected by adjusting the physical delay line in the non-reference FSRs. Since such an adjustment is possible only with positive values, a delay bias is

introduced into all antennas. The bias typically is set at a value at least equal to the maximum delay among the arrayed antennas. Later it is compensated for in the follow-on telemetry and radio metric processing by making proper adjustment of the Earth-received time tags of telemetry, Doppler, and ranging data.

In order to arrive at the correct determination of relative delay between two antennas, both sideband and carrier information are important. The reason is due to the 2π ambiguity in the phase difference from upper and lower sidebands. The sideband measurement alone can only point to a set of possible delays of modulo $1/(2*f_{sb})$, where f_{sb} is the sideband frequency. Among these values, only the true delay yields a stable correlation phase at the carrier frequency. All others will result in the carrier phase being monotonically increased or decreased, in modulo of 2π. Unfortunately, since the FSC does not perform carrier correlation, it relies on having delay residuals that fall within the 2π ambiguity error. The gross relative delays of the antennas in the system must be measured beforehand and stored in a table to serve as the beginning point for any observing pass. This table must be updated when any system configuration change is made that would affect these delays.

9.2.3 Combining

Combining is done in a straightforward way. The 16-MHz samples from different FSRs are weighted according to their relative SNRs. These weights can be determined by measurement of the SNRs derived at each antenna or by an analysis of the actual correlation results. The FSC presently uses the first method. The system allows for disabling certain inputs when a signal is not detected, so that the noncontributing elements will not degrade the gain performance.

9.3 Results

Results of field demonstrations at Goldstone with missions currently in flight are discussed in this section. Emphasis is placed on the array gain for telemetry and radio metric data.

9.3.1 Telemetry Array Gain

Figure 9-8 shows the measurements of individual data SNRs (P_d/N_o) at each of the two Goldstone 34-m antennas and at the combined signal during one of the 1998 Mars Climate Orbiter cruise tracks in July 1999. The profiles vary as a function of time because of the changing elevation. An average array gain of 2.9 ± 0.2 dB was observed, as compared to a 3.0-dB theoretical improvement. The 0.1-dB difference is attributed to error in the correlation in the presence of noise as well as to signal-processing loss in the hardware.

Laboratory measurement with calibrated test signals puts an upper limit of SNR degradation, as caused by hardware, within 0.2 dB.

Figure 9-9 presents results from an array of maximum configuration. It employs all operational antennas available for X-band deep-space support at Goldstone. The track was conducted with the Saturn-bound Cassini spacecraft in August 1999. Relative to the performance of the 70-m antenna, the array yielded a gain of 1.8 ± 0.6 dB. Theoretical improvement would have been 2.0 dB.

An additional test experiment was conducted in February 2002 using three 34-m antennas at Goldstone, also observing the Cassini spacecraft at X-band. Figure 9-10 presents the results of this array. Relative to the performance of Deep Space Station (DSS) 24, which was used as the reference, the array yielded a gain of 6.0 ± 0.3 dB. Theoretical improvement would have been 5.9 dB. Figure 9-11 shows the phase corrections that were applied during this experiment to DSS 15 and DSS 25 to bring them into alignment with DSS 24. The remarkably low level of variation of this phase correction is undoubtedly due to the very good weather conditions that prevailed on this day. Typical phase variation is as much as 20 times what is seen here.

9.3.2 Radio Metric Array Gain

Ranging measurements also were obtained in July 1999, on a different track with Cassini using an array of two 34-m antennas. Surprisingly, the realized gain for ranging was not the same as for telemetry. A 1.6 ± 0.3 dB gain was

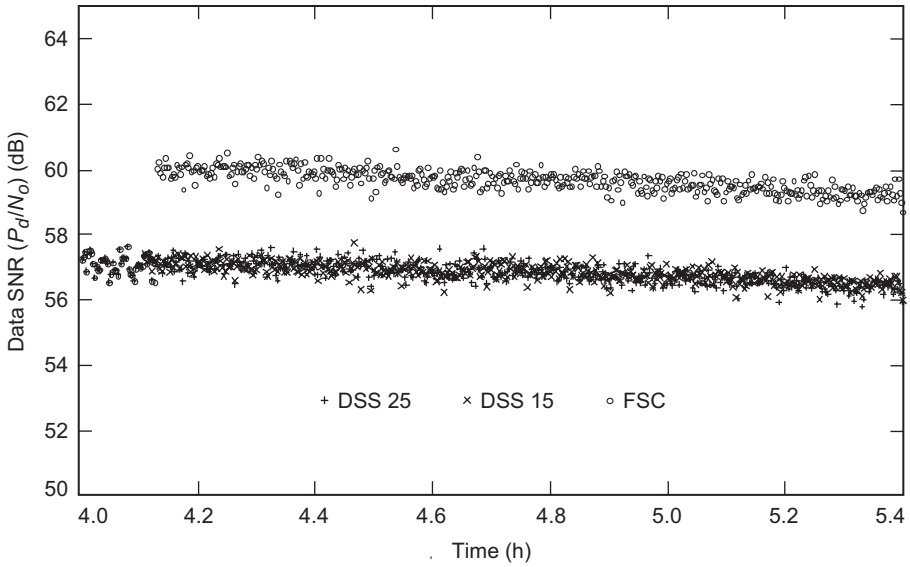

Fig. 9-8. Two-antenna arraying with 1998 Mars Climate Orbiter.

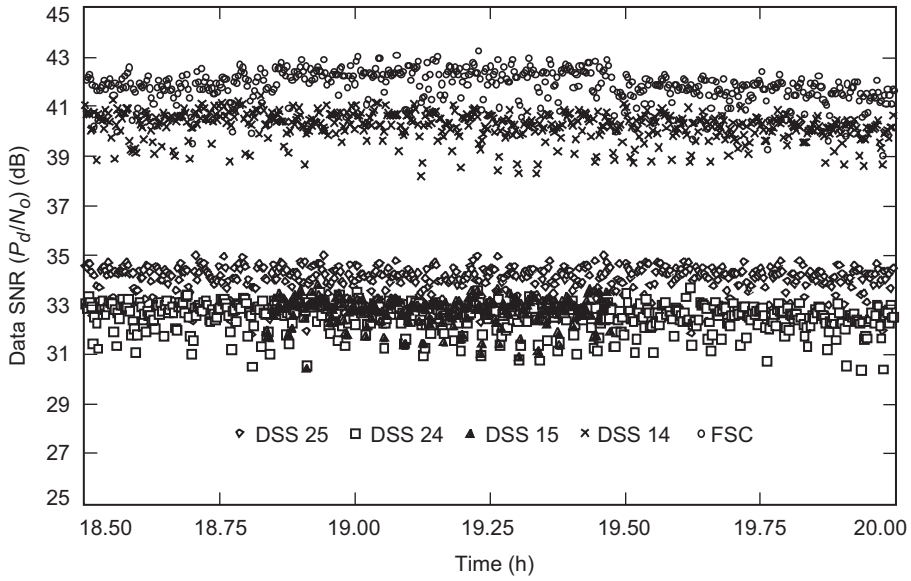

Fig. 9-9. Four-antenna arraying with Cassini.

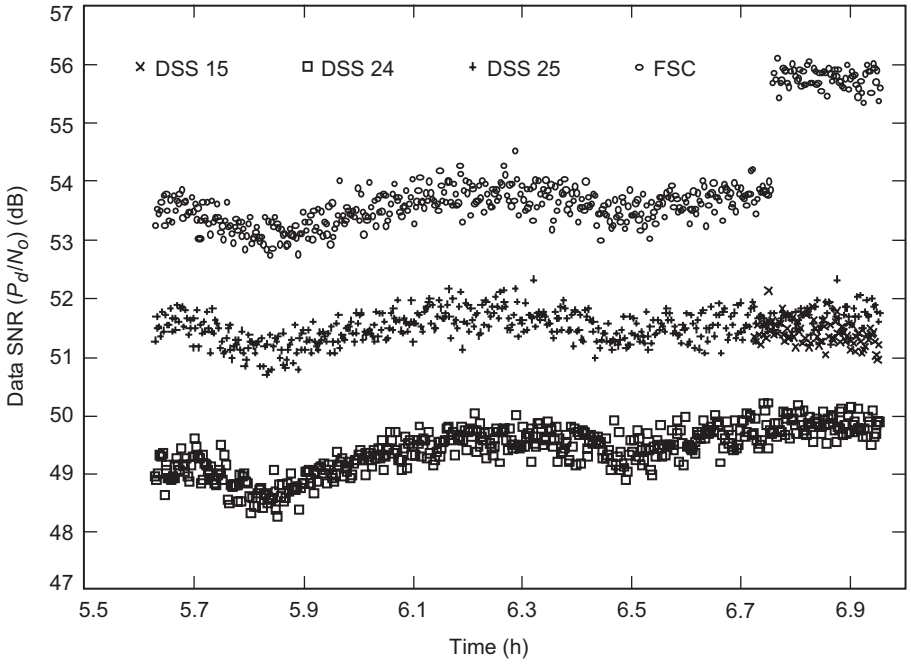

Fig. 9-10. Three-antenna arraying with Cassini.

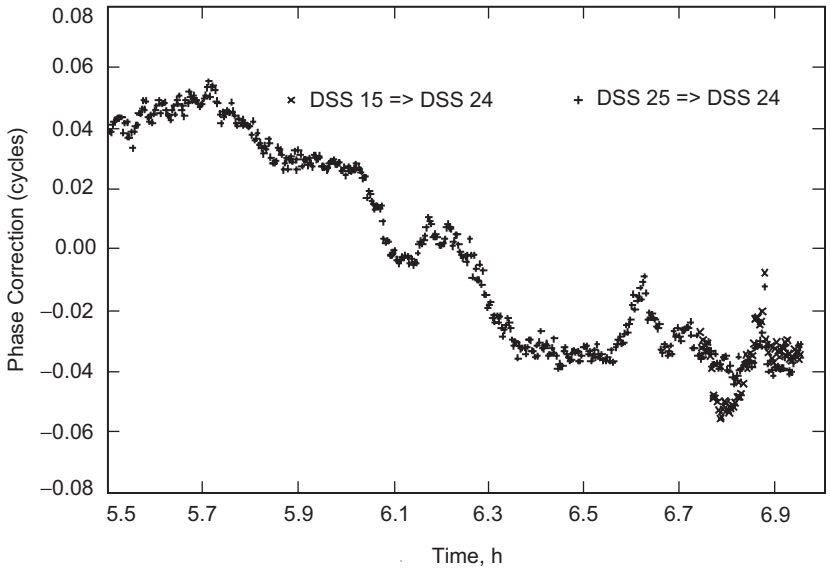

Fig. 9-11. Phase corrections for three-antenna arraying with Cassini.

measured relative to 2.4 dB predicted, which was confirmed by a measured 2.3-dB gain on telemetry. The most likely cause is the fact that the ranging component lies much further away in frequency from the carrier, as compared to the sideband component. In the presence of noise and ever-changing Doppler frequency, the error in the phase and delay estimation at the position of the 22-kHz sideband is magnified when extrapolated to the position of the 1-MHz ranging signal.

References

[1] D. W. Brown, H. W. Cooper, J. W. Armstrong, and S. S. Kent, "Parkes-CDSCC Telemetry Array: Equipment Design," *The Telecommunications and Data Acquisition Progress Report 42-85, January–March 1986*, Jet Propulsion Laboratory, Pasadena, California, pp. 85–110, May 15, 1986. http://ipnpr.jpl.nasa.gov/progress_report/

[2] D. W. Brown, W. D. Brundage, J. S. Ulvestad, S. S. Kent, and K. P. Bartos, "Interagency Telemetry Arraying for Voyager–Neptune Encounter," *The Telecommunications and Data Acquisition Progress Report 42-102, April–June 1990*, Jet Propulsion Laboratory, Pasadena, California, pp. 91–118, August 15, 1990.

http://ipnpr.jpl.nasa.gov/progress_report/

[3] J. W. Layland, F. D. McLaughlin, P. E. Beyer, D. J. Mudgway, D. W. Brown, R. W. Burt, R. J. Wallace, J. M. Ludwindki, B. D. Madsen, J. C. McKinney, N. Renzetti, and J. S. Ulvestad, "Galileo Array Study Team Report," *The Telecommunications and Data Acquisition Progress Report 42-103, July–September 1990*, Jet Propulsion Laboratory, Pasadena, California, pp. 161–169, November 15, 1990.
http://ipnpr.jpl.nasa.gov/progress_report/

[4] J. I. Statman, "Optimizing the Galileo Space Communication Link," *The Telecommunications and Data Acquisition Progress Report 42-116, October–December 1993*, Jet Propulsion Laboratory, Pasadena, California, pp. 114–120, February 15, 1994.
http://ipnpr.jpl.nasa.gov/progress_report/

[5] T. T. Pham, S. Shambayati, D. E. Hardi, and S. G. Finley, "Tracking the Galileo Spacecraft With the DSCC Galileo Telemetry Prototype," *The Telecommunications and Data Acquisition Progress Report 42-119, July–September 1994*, Jet Propulsion Laboratory, Pasadena, California, pp. 221–235, November 15, 1994.
http://ipnpr.jpl.nasa.gov/progress_report/

[6] Rogstad, D. H., "Suppressed Carrier Full-Spectrum Combining," *The Telecommunications and Data Acquisition Progress Report 42-107, July–September 1991*, Jet Propulsion Laboratory, Pasadena, California, pp. 12–20, November 15, 1991.
http://ipnpr.jpl.nasa.gov/progress_report/

[7] D. Fort, *Array Preliminary Design Review* (internal document), Jet Propulsion Laboratory, Pasadena, California, January 1998.

[8] K.-M. Cheung, "Eigen Theory for Optimal Signal Combining: A Unified Approach," *The Telecommunications and Data Acquisition Progress Report 42-126, April–June 1996*, Jet Propulsion Laboratory, Pasadena, California, pp. 1–9, August 15, 1996.
http://ipnpr.jpl.nasa.gov/progress_report/

[9] R. Kahn, *Array Preliminary Design Review* (internal document), Jet Propulsion Laboratory, Pasadena, California, January 1998.

[10] R. J. Dewey, "The Effects of Correlated Noise in Intra-Complex DSN Arrays for S-Band Galileo Telemetry Reception," *The Telecommunications and Data Acquisition Progress Report 42-111, July–September 1992*, Jet Propulsion Laboratory, Pasadena, California, pp. 129–152 November 15, 1992.
http://ipnpr.jpl.nasa.gov/progress_report/